

Friedrich H. Balck

## Radiaesthesia as an Important Tool for Physical Experiments - Part 3 Structures around masses, variations caused by excitations, and effects of noble gases



Many persons with enhanced perceptive abilities can detect structures around real matter [1-6]. Presumably, subtle matter [7] is somehow coupled with real, visible matter. The resulting questions are thus whether or not and when which relationship exists between the real mass and the magnitude of the associated structures, and how the structures react with external effects.

- In a series of experiments with various bodies (of different material, mass, and shape) it has been demonstrated that an orbital or spherical shell structure is present around every physical body, and that its volume is proportional to the mass.
- Bodies of the same kind can react with one another if their orbitals are in mutual contact or if they overlap.
- In a second series of experiments, an internal substructure has in part been determined within a structure. The size of the structures varies as a result of external excitation, for instance, by acoustic or electromagnetic waves.
- From experiments performed in a vacuum and with various gases, it has been concluded that certain gases are necessary for the establishment of the perceptible structures.
- In particular, noble gases and hydrogen are evidently decisive as intermediates between real and subtle matter.



Figure 01a-b: The infructescence of a dandelion and the pond skater possess a soft external structure.

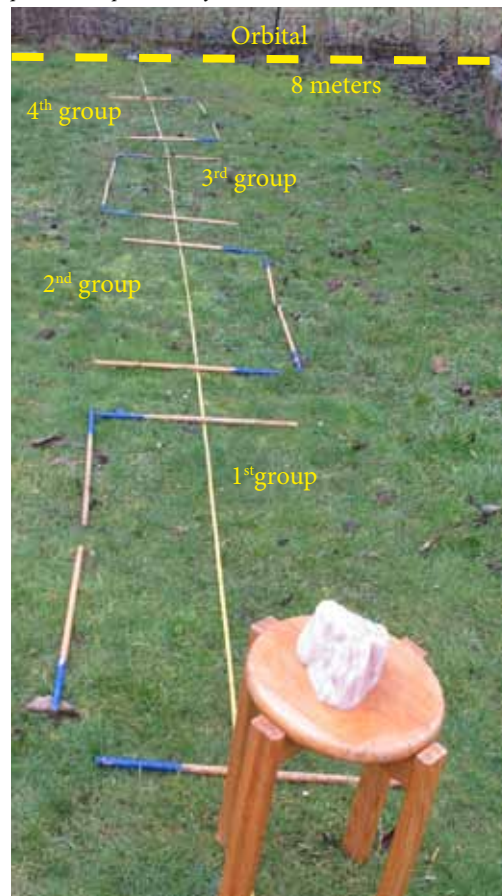


Figure 02: Soapstone, 3100 g: The observed structure with marked boundaries consists of four groups and an external spherical shell over a distance of 8 metres.

### 1. External spherical shell (orbital)

In the visible world, more substantial objects with surrounding lower-density structures are well known, for instance, **dandelion blossoms** going to seed and **pond skaters** (Gerridae). In these cases, more or less solid objects are surrounded by soft elements (figure 01, figure 02). The initial experiments began with a **soapstone** specimen with a mass of 3100 g (figure 03). This stone consists of talcum or steatite,  $Mg_3[Si_4O_{10}(OH)_2]$ , and contains large quantities of oxygen and silicon as  $Si_2O_5$ , as is the case with rose quartz. The stone was situated on a wooden stool in a garden which was essentially free of electromog. [8] The observed structure consists of a spherical shell with a radius of about 8 metres and several (four) groups, whose boundaries are marked with wooden poles on the lawn. In each group, four elements with distinguishable qualities and with an average width of about 20 cm were observed (figure 03).

#### Our initial hypotheses:

- Every physical body is surrounded by **structured, invisible matter** in the form of orbitals, that is, spherical shells (figure 04).
- **Sensitive persons** can perceive these structures.
- **Orbitals** around two similar bodies (identical material) **can coalesce**.
- The structures contain **information on the material** of the test body.
- This fact allows selective divining processes.



Figure 03: The internal group includes four elements approximately 20 cm in width and with different perceptible qualities.

### 1.1 Overlapping or superposing of orbitals

If two bodies of the same material are located so far apart that the associated orbitals are not in mutual contact, each object has its own separate orbital. However, if the two bodies are brought more closely together, the orbitals coalesce to form a single, joint orbital (figure 05).

### 1.2 Resonance

If bodies have a common, joint orbital, additional **resonance structures** occur. These structures are three-dimensional, tubular “hoses”. The cross-sections of a few such hoses are outlined on the grass with white and yellow metre sticks, as illustrated in figure 06.

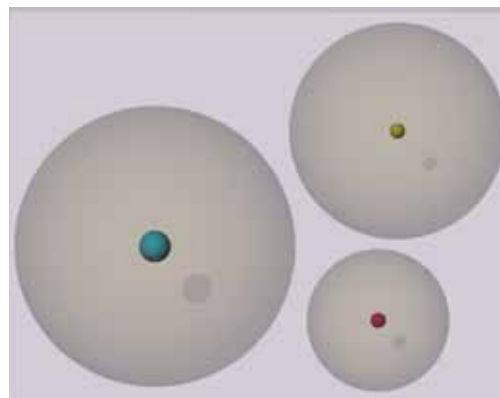


Figure 04: Extended concept: Every physical body is surrounded by orbitals of invisible matter (spherical shells with content).

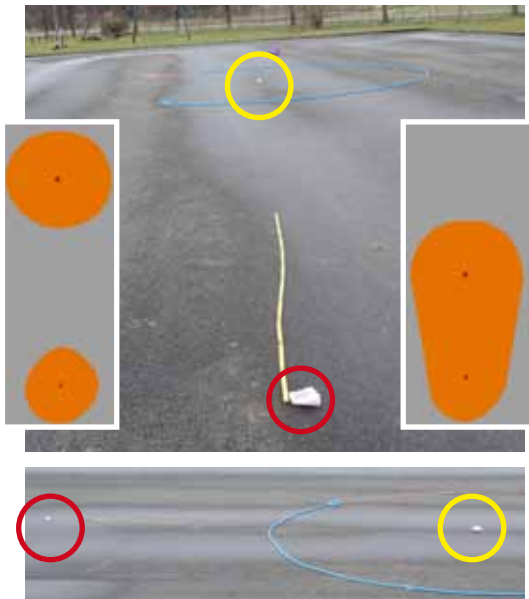


Figure 05a-d: Two stones of rose quartz are situated so far apart on a parking lot that their orbitals are not in contact. The orbital of one stone (920 g, yellow circle) has a radius of 3.1 m and is identified by a blue string. The orbital of the other (418 g, red circle) has a radius of 2.2 m. This is somewhat larger than the marked scale. The two-dimensional cross-sections through the orbitals are shown to scale in the diagram on the left-hand side. The situation which results if the front stone is moved backward by a few metres is illustrated in the figures on the right and below. The two orbitals then overlap.

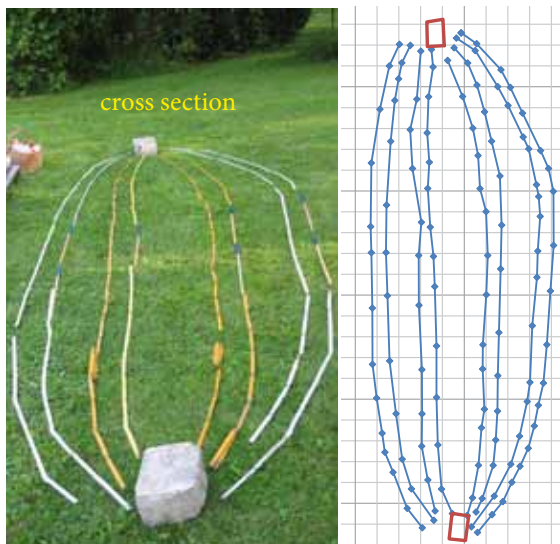


Figure 06a-b: Two limestones, each with a mass of 18 kg, are located approximately 5 metres apart. The resonant structure is about 1.6 m wide. The true-to-scale grid has a spacing of 20 cm.

### 1.3 Mass of the bodies and radius of the orbitals

In order to determine how the **volume** of the orbitals and the **mass** of the associated body are related, experiments have been performed with different materials, masses, and shapes (figure 07 a-f). The relationship thus found evidently obeys simple laws: **The volume of the orbital is proportional to the mass of the body.**

For coarse matter, the density is calculated from the mass and volume. This relationship evidently applies to subtle matter as well. A volume of subtle matter corresponds to every mass of coarse matter (figures 08-09). As indicated by experimental results, however, the proportionality factor, that is, the “density of subtle matter” within the orbital, also depends on external effects. The results of our experiments indicate that the orbitals can grow or shrink, for instance, as a result of acoustic or electromagnetic excitation by technical instruments. Cosmic or natural terrestrial excitation can also exert an influence.

a) For **real (coarse) matter** with volume **V**, mass **m**, and density **ρ**, the following relationship applies:

$$V = \frac{1}{\rho} \cdot m$$

b) Observation with “**subtle matter**” structures: The volume **V** of the spherical orbital is proportional to the mass **m** of the included body plus an additive constant **c2**:

$$V = c_1 \cdot m + c_2$$

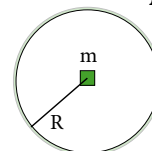
Since the relative measuring error is very much larger in the case of the radius than for the mass, the use of the measured value of the radius is better suited for plotting the proportionality than the use of the calculated volume. For this purpose, the cube root of the mass is first calculated.

$$V \sim R^3 \quad | \quad R^3 \sim c_1 \cdot m + c_2 \quad | \quad R \sim \sqrt[3]{c_1 \cdot m + c_2}$$

In the case of proportionality, the plots must yield straight lines.

$$R \sim \sqrt[3]{m}$$

Cross-section through the orbital



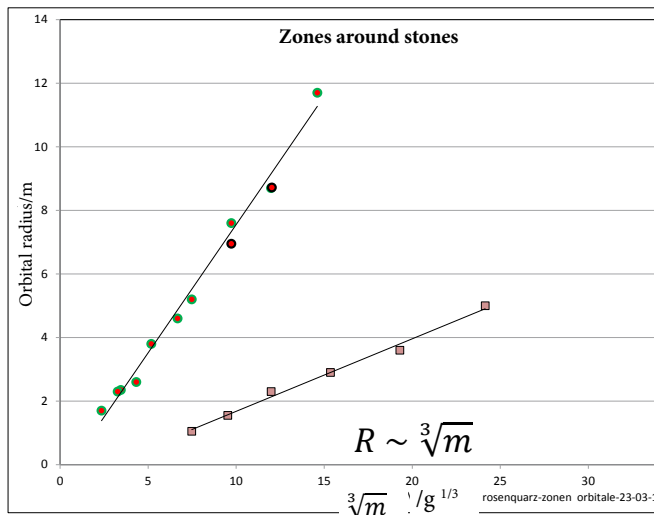
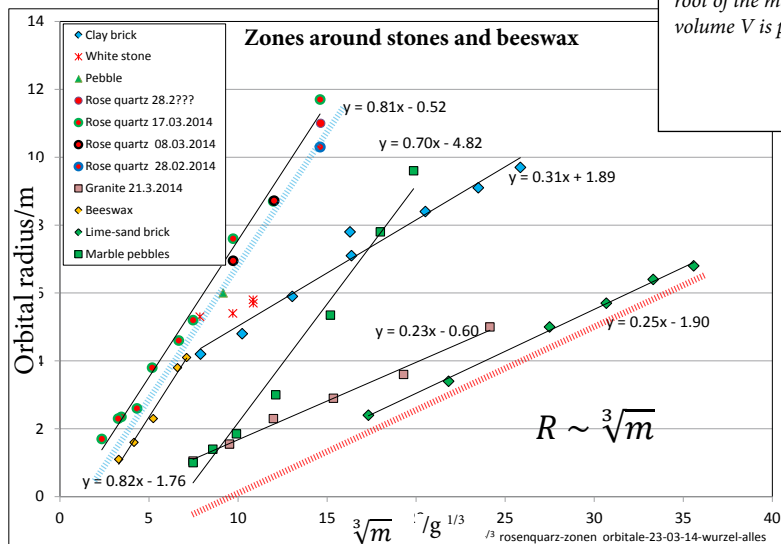
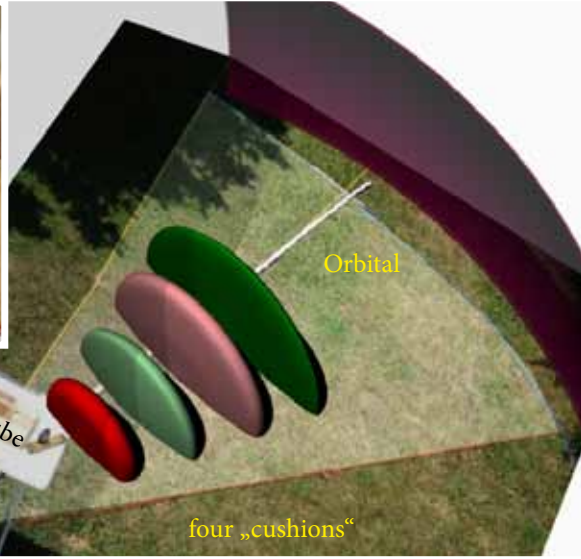


Figure 07 a-f: (top) various masses (mass in grams)  
 Top: Marble gravelstone, rose quartz, calcareous sandstone  
 Bottom: Brick, beeswax, and granite

Figure 08: (m.) The radius of the orbital is plotted as a function of the third root of the mass, for selected stones. The two trend lines indicate the existence of linear dependencies as well as differences in slope.

Figure 09: All observations are plotted in a single diagram. Two types of trend lines exist. Each of these trend lines describes the behaviour during the respective series of measurements very well. Thus, the radius of the orbital  $R$  is proportional to the third root of the mass  $m$ ; that is, the enclosed volume  $V$  is proportional to the mass  $m$ .





## 2. Excitation of hollow bodies

In the preceding section, the structures have been treated as **massive bodies**. In the contrast to this consideration, additional elements are present in the case of **hollow bodies**, such as spheres or tubes. [9]

For the following investigations, a **quartz tube** 50 cm in length, 9 cm in diameter and with a mass of 850 g has been employed (figure 10). In the present case, the tube was located on a table in a spacious garden free of electrosmog and was oriented along the north-south axis. Thus, it was possible to investigate structures with radii of many metres. As in the case of massive bodies, a spherical shell (orbital) is also present in the case of the tube. The observed radius was 5.5 m in length. A sensitive observer can find several pillow- or cushion-shaped structures within this spherical shell if he moves from the outer edge of the shell to the midpoint.

### 2.1 Arrangement of the structures

As indicated by the results of observations, the structures are arranged in several sectors within the spherical shell. The respective groups in turn are arranged symmetrically with respect to the axis of the tube. A group consists of four “cushions” with distinguishable qualities (represented diagrammatically in different colours in figure 12). Each “cushion” is surrounded by a perceptible “skin”. This skin may possess a structure similar to that of a

Figure 10: (left) A quartz tube 50 cm in length and 9 cm in diameter is located on a table in a garden.

Figure 11: (centre) An AA flashlight monocell is located near the opening of the quartz tube. The tube can thus be excited.

Figure 12: (right) The contours of the observed structures are marked by coloured strings on the lawn. In the computer-graphics diagram, the surrounding orbital (spherical shell) is indicated schematically in violet. A group with four “cushions” of different qualities is also shown.

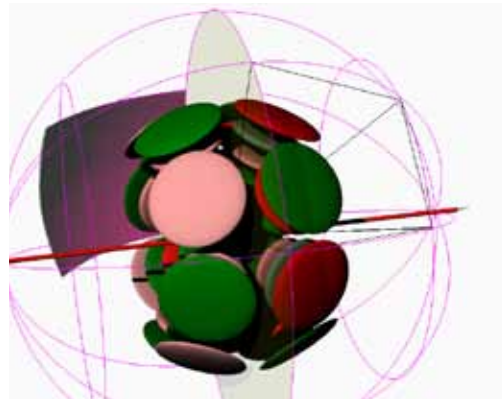


Figure 13: In this rough sketch, several selected structures within the spherical shell are illustrated schematically: red - axis of the tube; grey - “equatorial plane”; violet - spherical shell, and groups of “cushions”.

soap bubble. The manner in which eight such groups, respectively, may be arranged above and below an “equatorial plane” is illustrated in figure 17. With such an arrangement, a certain **condition** seems to apply: **Only cushions with different qualities can be immediate, nearest neighbours.**

## 2.2 Time-dependent behaviour during external excitation

The arrangement and number of cushions depend on external effects.

**If a comparatively weak excitation (such as a small magnet) is actuated, the variations occur so slowly that they attain their new state of equilibrium only after many seconds to several minutes.**

For the purpose of radiaesthetic observation, a douser moved inward along a measuring scale consisting of levelling staves at intervals of one minute each and committed his results to protocol (by dictaphone or video recording).

The excitation was initially introduced in the form of acoustic or electromagnetic waves from a small loudspeaker (headphones) and from a mobile telephone in the stand-by condition.

For further investigations, polarised objects such as flashlight monocells, magnets and even plant stems also proved to be well suited for use as sources of excitation, if they are placed in or near the tube opening (figure 11).

The **same extraordinary behaviour** is observed during many experiments: A **group consisting of four “cushions”** first travels outward toward the outer edge of the spherical shell. After a certain period of time, a further group, likewise consisting of four “cushions”, begins at the centre and then moves outward. If the external

excitation persists, this new group likewise moves outward, and another new group then begins to form at the centre. “Cushions” which already exist become more densely packed at the edge of the spherical shell. However, the “cushions” always remain at a certain distance from one another.

## 2.3 Acoustic excitation

In figures 14 and 15, a recorded alternation of this kind is plotted over a period of 20 minutes for an excitation at a frequency of 305 Hz from a small headphone loudspeaker.

**Observation:** The first group (blue) moves toward the outer edge at a distance of 5.5 m within a period of a few minutes, whereas the other groups (green to brown) begin to form much later and do not move as much. The groups appear to be mutually coupled in some way: At 18:37, the groups indicated in red and green exhibit similar variations.

## 2.4 Excitation by polarised objects

If a freshly cut **plant stem** is inserted into the tube, the resulting effect on the structures depends on the orientation. If the root end of the stem points toward the south, the structures grow; in the opposite case, the structures shrink. With the use of such an exciter, the

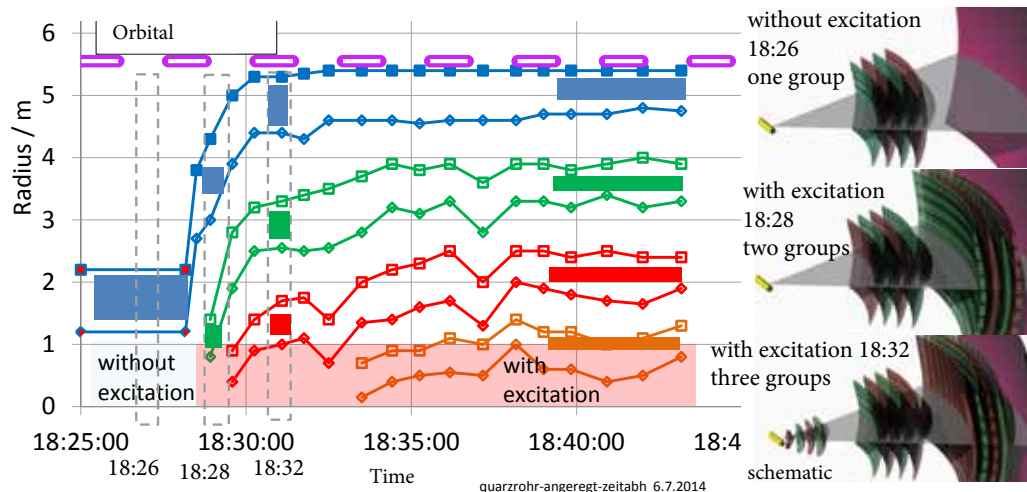


Figure 14: (right): The variation of the observed positions with time has been plotted for the four groups, blue, green, red, and brown, first without and then with excitation (pink bar over the axis of time). The indicated dashed frames belong to the adjacent computer graphics.

Figure 15 a-c (left): Without excitation, only one group with four “cushions” is present. With excitation, a second group first appears, and then a further group appears. The groups thereby move toward the outer shell (indicated schematically).

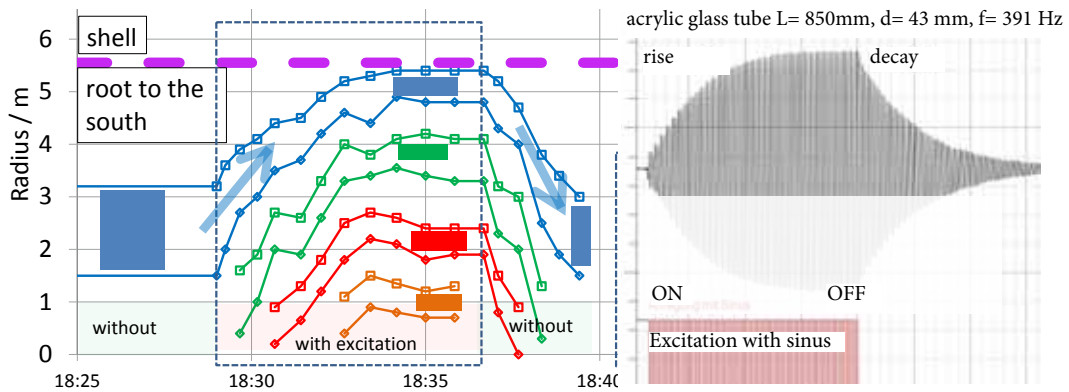


Figure 16: (left) A plant stem has been inserted into the quartz tube and then removed seven minutes later.

Figure 17: (right) For comparison, the variation of the loudness (volume) in an acoustic resonator (a tube such as an organ pipe) has been plotted as a function of time after brief excitation at the resonant frequency. The loudness initially increases gradually to a maximum and then decreases slowly after switching off (transient build-up and decay).

decay characteristics can also be studied.

The manner in which the groups initially grow after introduction of the stem, and then shrink or disappear some seven minutes later after removal of the stem, is shown in figure 16. In this context, the associated time constants evidently differ: **The structures decay faster than they grow.**

For comparison, the **behaviour of a resonator** (such as an organ pipe or similar tubular object) known from classical acoustics is illustrated in figure 17. The resonator is excited at its resonant frequency by an external signal from a small loudspeaker. The signal is switched on, and the loudness (volume) is then measured with a microphone. The loudness gradually increases and attains a maximum. The signal is then switched off, and the loudness decreases. In this case, too, the associated response and decay times may differ. Evidently, the behaviour of the structures present around the quartz tube with time is similar if it is excited by a plant stem. The experiment with the “organ pipe” evidently involves oscillatory energy, which is stored in the tube. Hence, the **structures present around the quartz tube may possibly act as an energy-storage device.**

If the direction of the plant stem is reversed, that is, if the root end of the stem now points toward the north, the structures shrink. In the case of a bar magnet (such as a weakly magnetised jack-

knife), the orientation also determines whether the structures grow and multiply, or whether they shrink and decay.

In figure 19, the behaviour of the structures is plotted on the left for the case of the plant stem, and on the right for the bar magnet. In both parts of the figure, both growth and shrinkage are observed.

The results plotted in figure 16 for the quartz tube and for the plant stem are re-plotted in figure 20 for both directions of polarisation, with and without excitation. The light blue horizontal bar is intended to symbolise the initial condition for growth as well as shrinkage of the first group. It may be assumed that this condition is established by natural excitation caused by cosmic or terrestrial effects. In the case of artificial excitation with a polarised object, superposition of natural and artificial effects may result in mutual **reinforcement or extinction**, as dictated by the orientation.

The observations with the quartz tube can then be compared with the behaviour of **energy-storage devices**, which are charged or discharged through a conductor with a certain resistance. The variation of the voltage on an energy-storage device (a low-pass filter, a combination of a resistor and a capacitor) is plotted in figure 21. The value follows the input voltage (indicated in green), but with a certain shift of the slopes along the time axis.

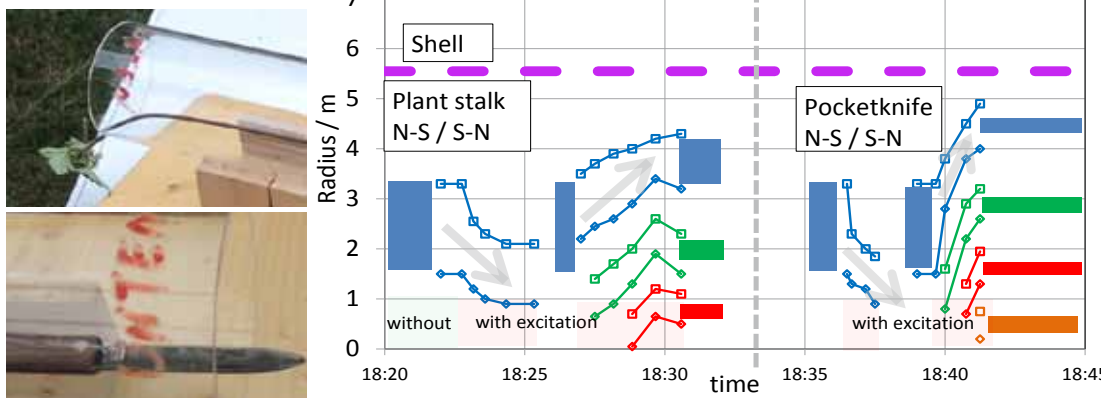


Figure 18 a-b: (left) Two possible exciters are illustrated here: a plant stem (above) and a weakly magnetised jack-knife (below).

Figure 19: (right) The position of the structures has been plotted as a function of time for the plant stem (left) and for the jack-knife (right), each for orientations in both opposite directions. If the root end of the stem points toward the north, the structures shrink; if it points toward the south, the structures grow and increase in number. In the case of the jack-knife, the behaviour is analogous.

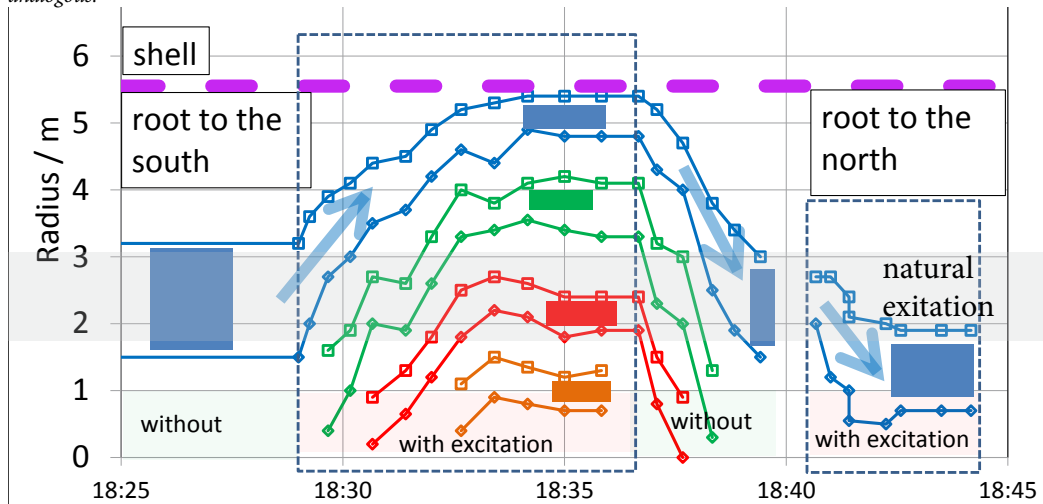


Figure 20: (left) A plant stem is situated in the tube, as illustrated in figure 16; with this orientation, the structures grow. (right) If the orientation of the plant stem is reversed, the structures shrink. The light blue bar in the middle is intended to symbolise average natural excitation. If natural excitation and artificial excitation are mutually superposed with the corresponding polarity, the combination can result in stronger or weaker excitation, respectively.

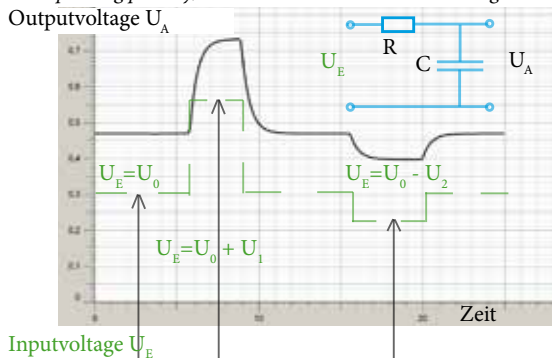


Figure 21: With alternating excitation, the size of the "cushions" behaves in a manner similar to that of the output voltage from a capacitor with a resistor (low-pass filter, energy-storage device).

- Examples of excitation
- sound
  - EM-waves
  - electric devices
  - batteries
  - magnets
  - plant stalks
  - living creatures
  - cosmic waves

### 3. Effect of noble gases

Several years ago, the authors had already observed that the perceptible effect of flowing water in a coil of pipe or tubing in the presence of alternating magnetic fields can be attenuated, if the coil is placed in a **vacuum chamber**, and the chamber is then evacuated. [10]

The **perceptible effect** is not observed again until **air** or very **small amounts of noble gases**, such as neon, are introduced into the vacuum chamber.

In order to determine this influence **quantitatively as well as qualitatively**, experiments have been performed with rotating magnets. In tests of this kind, the size of the observed structures depends on external effects, such as the rotational speed and sense of rotation. As expected, the **composition of the gases** present around the rotating object should also be decisive for the results.

#### 3.1 Rotating magnet in air

A small disc-shaped ferrite magnet is fastened to the end of a round wooden rod or pole. The magnetic axis is oriented in the same direction as the axis of the rod (figure 22a). [11] An extremely slow-running geared motor with various speed settings is coupled with the other end of the rod (figure 22b, figure 24). At this distance, the electric motor and the ferrite magnet are sufficiently well isolated from one another. Very low rotational speeds from 10 min<sup>-1</sup> to 0.001 min<sup>-1</sup> can thus be selected.

The entire set-up is positioned horizontally and located in an electrosmog-free garden. The structures found during the rotation of the magnet are indicated by coloured strings on the lawn (figure 22b) and can thus be measured.

These structures are **toroidal** and **club-shaped orbitals**, whose arrangement resembles that of **spherical functions** (figure 23a).

The spatial objects thus found all exhibit a two-shell structure (figure 23b). These objects are located above and below the equatorial plane of the rotational axis, regardless of whether the magnet is at rest or in motion.

However, the size of the toroids varies with the rotational speed. Furthermore, this variation occurs counter-currently; that is, if the toroids on one side grow, those on the other side shrink (figure 25).

#### 3.2 Rotating magnet in the absence of air or other gases

If the magnet rotates in a vacuum, no toroids can be found.

##### 3.2.1 Air as a transmitter of sound waves

If an electromagnetic door-bell (figure 26, from the mid-twentieth century) is placed in a vacuum chamber, and the air is pumped out, the loudness (volume) of the externally audible sound decreases as the air pressure in the chamber decreases (figure 27). If the chamber is refilled with air, the loudness increases to a maximal value (saturation). This experiment demonstrates that a **medium**, such as air, is necessary for the propagation of sound waves.

#### 3.3 Rotating magnet in noble gases

As described in section 3.1, a flat disc-shaped magnet is again allowed to rotate slowly about its magnetic axis [12], but this time in a vacuum chamber (figure 28). The radii of a torus have been measured as a function of the gas pressure for various noble gases as well as hydrogen in the chamber. At the beginning of each experiment, the chamber was evacuated. Defined quantities of a noble gas or hydrogen were then introduced into the chamber with a graduated syringe (for instance, 1 ml), and the radius of a torus was measured. This step was repeated several times up to a gas content of about 20 ml.

In comparison with the volume of the vacuum chamber (11 000 ml), the **quantity of gas involved here is very small**.

The results (figure 29) have been obtained from a very large number of measurements - and these measurements have been performed on different days. The radius of the torus is plotted as a function of the **added quantity of gas**. In agreement with the results of the experiments with the domestic door-bell, no structures are observed in a vacuum. No torus appears until a very small amount of gas has been introduced. The radius then increases to a **maximum** (saturation).

**Thus, a relationship has been quantitatively determined between noble gases and the size of perceptible structures.**

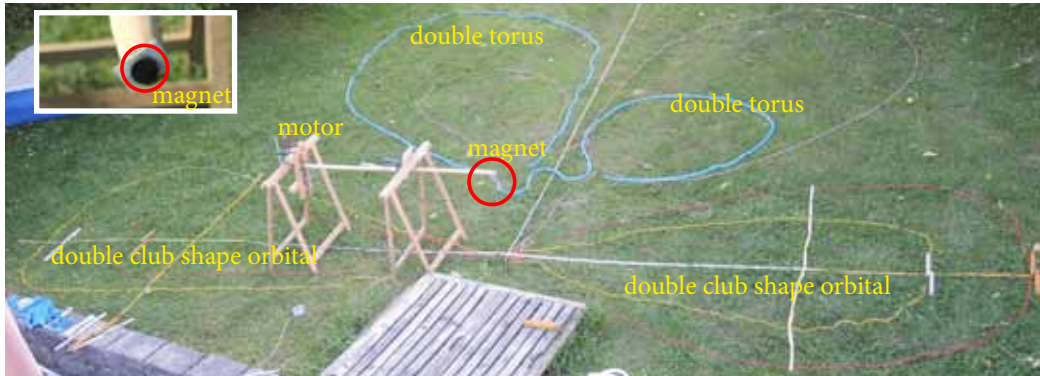


Figure 22a: (left) A flat bar magnet has been cemented to the tip of a wooden pole.

Figure 22b: The magnet and wooden pole are mounted on supports and can be rotated. The geared motor is attached to the left end of the wooden pole. In each case, the observed structures - a double torus and a double conical orbital - are marked with coloured strings.

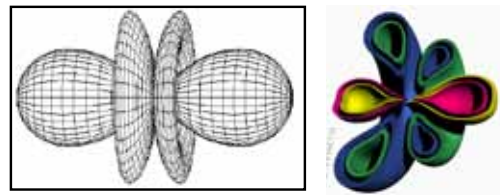


Figure 23a: (top): Spherical function

Figure 23b: (right) (schematic): The sizes of the observed two-shell structures above and below the equatorial plane are different.

Figure 24: (left) The geared motor has numerous speed settings. The specifications are referred to the rotational speed in  $\text{min}^{-1}$ . In this case, the flat bar magnet is fastened directly to the shaft. For the preceding experiment, a long wooden pole was situated between the motor and the magnet.

Figure 25: (bottom): A section through a double torus (eight measurements each) is illustrated for measurements at different rotational speeds and in both directions. The rotational speed was varied in the following steps: 4: 10; 3: 3; 2: 1; 1: 0,3  $\text{min}^{-1}$ . The torus grows with increasing rotational speed, but shrinks with decreasing rotational speed or during rotation in the opposite sense.

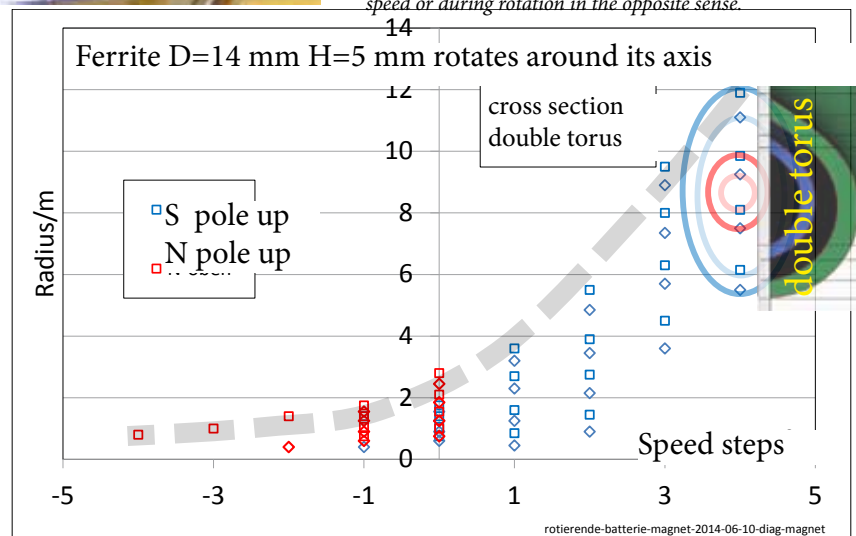




Figure 26: (left) An electromagnetic door-bell is placed in a vacuum chamber. A sound-level meter is located on the right-hand side of the chamber.

Figure 27: (l.m.): The measured loudness depends on the air pressure in the vacuum chamber. If air is admitted into the chamber, the loudness increases to a maximum (dashed line: saturation).

Figure 28: (r.m.): A flat neodymium bar magnet is mounted on the shaft of a motor. Both are located in a vacuum chamber.

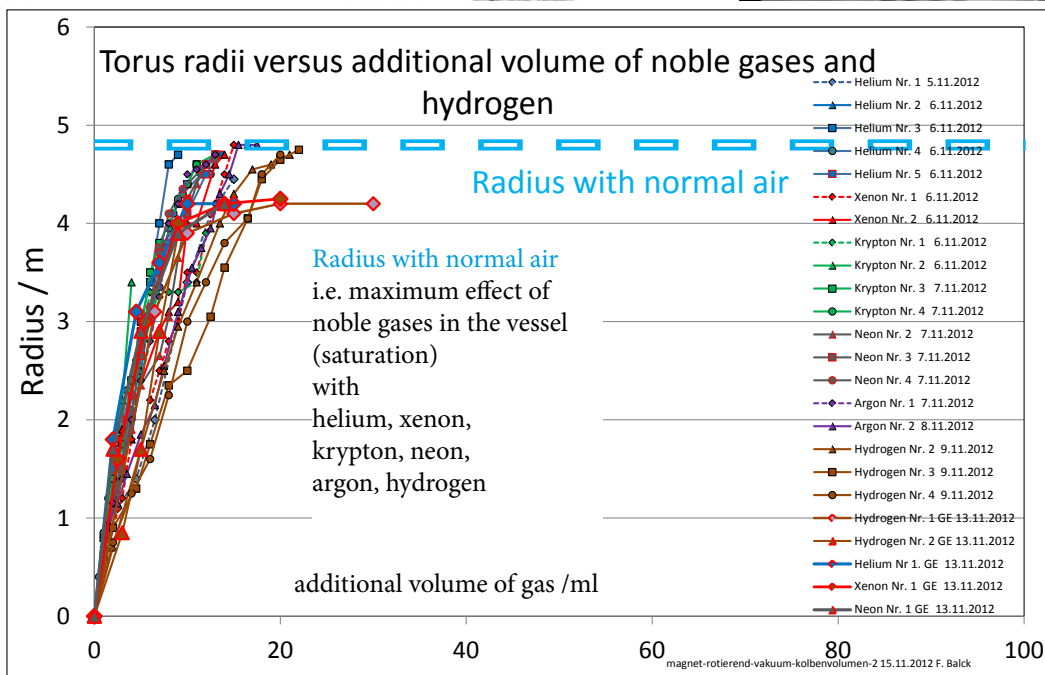
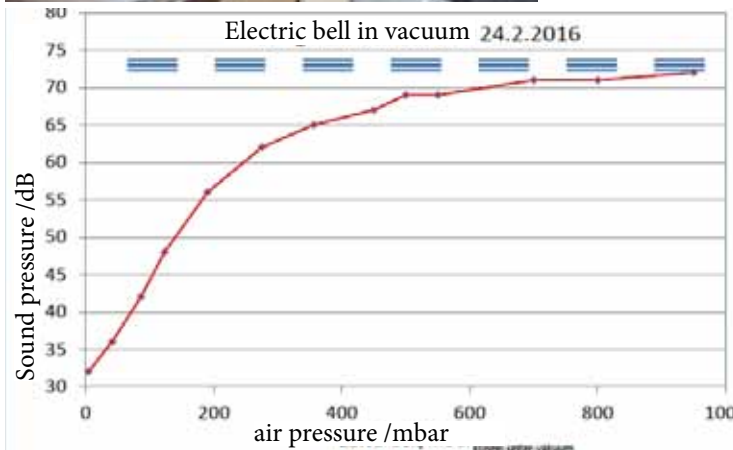


Figure 29: Torus radii are measured at different levels of filling with gas: helium, xenon, krypton, neon, argon, and hydrogen. By means of a syringe, the gas is introduced in quantities which are small in comparison with the volume of the vacuum chamber, that is, 11000 ml. No torus is observed under vacuum (1/1000th of atmospheric pressure). The structure does not form until a sufficient quantity of gas has been admitted into the chamber. The structure then grows to a saturation value (dashed line).

### 3.4 Quartz tube filled with noble gas

In the case of the quartz tube, too, the influence of noble gases can be demonstrated. [9] For this purpose, the quartz tube is sealed at both ends and connected to a vacuum pump as well as a gas-filling device. As in the preceding experiment with the rotating magnet, the outside and inside radii of the respective groups with the “cushions” are determined as functions of the **gas pressure**.

Each individual experiment begins with the near-vacuum state at about 1 mbar. The gas pressure is subsequently increased stepwise. A waiting period of several minutes was included between the gas-filling process and the measurement, in order to allow adjustment of the system to the altered conditions.

In figure 31, the growth of the “cushions” is plotted as a function of the degree of **filling with air**. At approximately 100 mbar (10 per cent of atmospheric pressure), the structure attains its maximal size with four groups. Below approximately 20 mbar, no “cushions” are observed.

If the tube is filled with neon (figure 32), the result is analogous to that observed with air, but with one important difference: The **structure already begins to form at about 1 mbar** and attains its saturation value at about 5 mbar.

Similar behaviour is observed upon **filling with helium**, as illustrated in figure 33. Thus,

the plotted result resembles that obtained with neon. At higher values of the pressure, an additional, fifth group appears. However, the size of the spherical orbital does not change.

In the case of two further noble gases, that is, **argon and xenon**, the radius of the spherical shell increases with increasing gas pressure (figure 34 and figure 35). At the same time, the number of groups increases to seven. Does a larger spherical shell offer more space for accommodation?

### 3.5 Comparison of various gases

In addition to the noble gases, the following gases have been investigated (see table):

- In the cases of **nitrogen, oxygen, and carbon dioxide**, no “cushions” have been found.
- However, a **spherical orbital** exists in these cases, too.
- **Hydrogen and gases which contain hydrogen** exhibit behaviour similar to that of neon, for instance.
- Among the five noble gases under investigation, the behaviour of **argon and xenon** differs from that of **helium, neon, and krypton**.
- **Radon** has not been investigated.
- In the cases of **argon and xenon**, the spherical orbital grows with increasing gas pressure.

Without additional excitation

Gas	outer shell	“cushions“
Oxygen	remains constant	no „cushions“
Nitrogen		
Carbon dioxide		
<b>Gases with hydrogen</b>		
Hydrogen	remains constant	changes with increasing gas pressure
Deuterium		
Butane/propylene/propane		
Water vapor		
Air		
<b>Noble gases</b>		
<b>Helium, neon, krypton</b>	remains constant	changes
<b>Argon, xenon</b>	<b>changes</b>	changes

Table: The effect of the gas pressure on the growth of the “cushions” and of the spherical orbital is considered for the case without additional excitation.



Figure 30: The quartz tube has been sealed air-tight above and below, and can thus be evacuated. By means of an appropriate filling device, the tube can then be refilled with gas. (An aluminum cylinder containing neon is illustrated in the figure.)

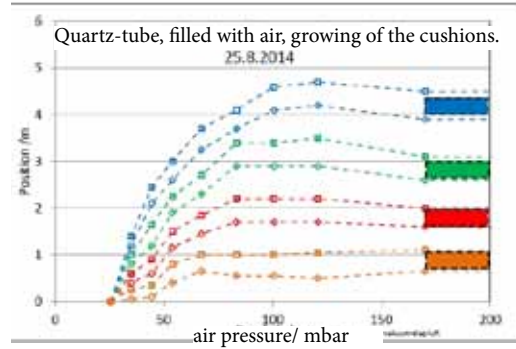


Figure 31: The quartz tube has been evacuated and refilled stepwise with air. Four groups of "cushions" are formed. These structures grow with increasing level of filling. A maximum is observed at about 100 mbar.

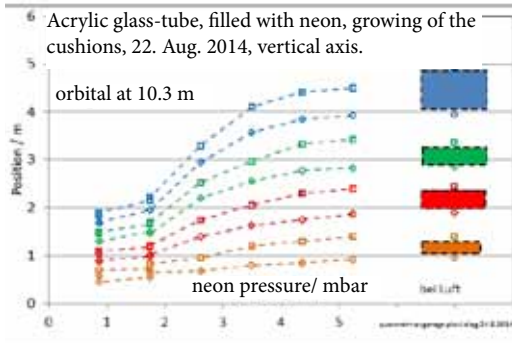


Figure 32: The acrylic glass tube has been evacuated and filled stepwise with neon: Four groups are already formed at a pressure of 5 mbar.

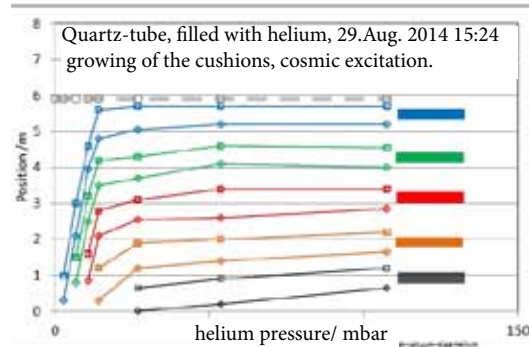


Figure 33: The quartz tube has been evacuated and filled stepwise with helium. The size of the spherical orbital (dashed line) does not change during this process. Furthermore, a fifth group is formed.

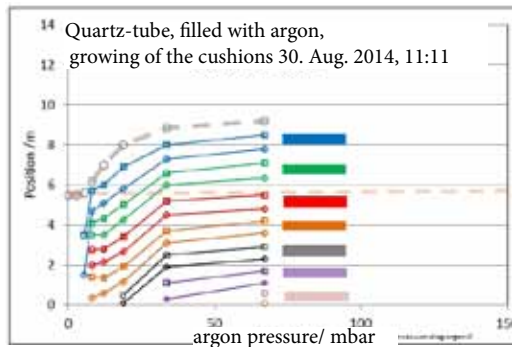


Figure 34: The quartz tube has been evacuated and filled stepwise with argon. The spherical orbital (dashed line) grows in this case. A total of seven groups with "cushions" are formed.

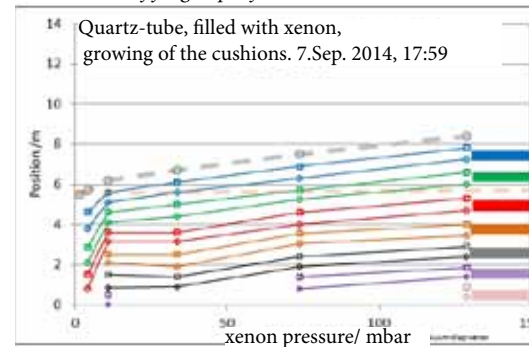


Figure 35: The quartz tube has been evacuated and filled stepwise with xenon. The spherical orbital (dashed line) grows in this case. A total of seven groups with "cushions" are formed.



Figure 36: Four water-filled balloons in different colours serve as object for visualisation of the cushion-shaped zones within a group.

### 3.6 Concerning the structure of the cushions

The cushion-shaped zones presumably consist of subtle matter. The “skin” of these structures evidently forms under the influence of noble gas atoms. The “cushions” possess **polar properties**. Repulsive forces prevail between cushions with different qualities. **Four different types of cushions** have been hitherto been distinguished.

### 3.7 Sudden disintegration as a result of interference

After clapping of hands or other acoustic impulses, the structures disintegrate. However, they subsequently re-establish themselves with the same time constants as those described in section 2.2. Thus, the effect of hand clapping is essentially a reset function or process on the time scale during the measurement.

### 3.8 Practical applications with LED lamps

The external shape of so-called **retrofit lamps** resembles that of conventional incandescent lamps (figure 37). These lamps have an external glass envelope and a threaded base

[13]. However, the internal components are LED elements rather than a tungsten filament. For experimental purposes, a glass tube has been fused to the tip of the glass envelope on a candle-flame-shaped LED lamp. During manufacture, a **gas with optimised heat-conducting properties** is introduced into the lamp. This gas can be pumped out through the attached glass tube. As a result of this measure, the otherwise **perceptible unpleasant effects associated with LED lamps disappear**, if the interior of the lamp is **evacuated or if carbon dioxide is present** there. On the other hand, if a very small quantity of a noble gas (such as argon) is introduced into the lamp, the usual structures again become clearly perceptible.

#### Consideration of errors

For our radiaesthetic observations, the position can be indicated only within  $\pm 5$  cm.

For the graphics with time axes, the beginning of the respective series of divining processes was indicated. The final data of this series (for instance, with four groups) may have been determined up to half a minute later.



Figure 37: Retrofit LED lamps have a glass envelope which is filled with a special gas for improving the heat dissipation. If this gas is pumped out and replaced by carbon dioxide, the perceptible effect which is observed during the operation of these lamps can be suppressed.

After filling the vacuum chamber with gas to a specified pressure, the leakage rate must be kept as low as possible. The increase in pressure was within the range of a few millibars per minute. Two mechanical manometers (coarse and fine) as well as an electronic multifunction instrument with a thermal conductivity sensor, among other features, were employed for the pressure measurements. The thermal conductivity sensor was calibrated for air, and not for noble gases. Consequently, deviations by up to 10 mbar may occur in the lower range up to 30 mbar in the case of noble gases.

#### 4. Conclusions

By means of the aforementioned experiments, we have entered a completely unexplored field of research with **three-dimensional structures** around objects.

The results of the measurements described in the preceding are only preliminary results and therefore require further proof. These initial experiments with **perceiving observers** should be followed by further experiments with „**seeing**” abilities.

The schematic diagram of the arrangement (figure 14) may be misleading and may result in the assumption that these are the only possible structures. However, this is not the case. Further structures exist, for instance, tori, club-shaped orbitals, and discs as separating elements between the groups.

As indicated by the example with the elephant [2], one cannot investigate something which one cannot perceive. Participation in the experiments by further observers in the research group would be desirable.

Evidently, the **spherical shells** are nearly static structures. However, the situation is entirely different in the case of the “**cushions**”: These structures behave **dynamically**; that is, they **grow or shrink** in correspondence with the excitation and also **rotate slowly** around the centre. An observer who moves stepwise through the structures and records the radii therefore obtains his values only at different times.

In contrast, a “seeing” observer would receive an **entirely different overall impression**

during a “**momentary observation**” and would also notice **additional details**.

The following questions thus result from the preceding considerations:

- What is the structure of the “cushions”?
- Does any flow occur?
- Do any of the “cushions” pulsate or rotate?
- At which location does a determination of the radii make sense?
- Where is the greatest spatial extent of the “cushions”?
- What external time-dependent effects occur?

These numerous questions illustrate and emphasise the complexity of the problem.

#### Physical conclusions

##### Orbitals

Every physical body is surrounded by spherical shells or orbitals which consist of subtle matter. The **volume** within these shells is **proportional to the mass of the body**.

**Mutual interactions** can occur among **neighbouring bodies of the same material**, if they are so close together that the **orbitals overlap**.

The orbital around a body includes **information concerning the material** of which the body consists. The size of the orbital depends on the natural or artificial **excitation** to which the body is subjected.

##### Cushions

The structures observed with the quartz tube include **cushion-shaped zones**, among other features. These “cushions” are arranged in **groups of four**. Upon external excitation, (for instance, by acoustic or electromagnetic waves, or by “**active**” objects, such as batteries, magnets, or plant stems) the structures can grow or shrink within the spherical orbital.

The **reaction time** after actuation of an excitation is of the order of minutes. After discontinuation of an excitation, the system likewise requires a period of minutes before reverting to the initial condition. Thus, the

behaviour of the system resembles that of an **acoustic resonator** which is excited at its resonant frequency for a brief period.

However, **mechanical disturbances** (such as clapping of hands) can cause immediate collapse or disintegration of the additional groups within a period of seconds. After such an interruption, the additional groups re-establish themselves immediately, provided that the excitation persists, albeit with the aforementioned longer reaction time.

From the experiments with the **noble gases**, it is quite obvious that the cushion-shaped structures can form only if a **sufficient concentration of noble gas** is present over the entire distance **from the object to the spherical shell**. This behaviour resembles that of the domestic door-bell in the vacuum chamber. The ringing sound can be heard only if the gas necessary for the propagation of sound is present over the entire distance from the door-bell to the observer.

On the basis of the preceding observations (clapping of hands and noble gases) it may be presumed that the shells which surround the “cushions” contain **clusters of noble gases**, for instance. These clusters disintegrate (in much the same way as soap bubbles) if they are subjected to a mechanical disturbance.

Our experiments have shown that structures consisting of subtle matter exist in the region which surrounds physical bodies. These structures evidently possess definite shapes which can be described mathematically. The structures behave dynamically in correspondence with the excitation to which they are subjected. Thus, every divining process is evidently a momentary observation, a kind of “snapshot”.

Prof. Dr. Friedrich H. Balck  
Siebensternweg 2  
38678 Clausthal-Zellerfeld

www.biosensor.de  
22.01.2017

#### References

- root =<http://www.biosensor-physik.de/biosensor/>  
or from web-archive: root= [http://web.archive.org/web/\\*/http://www.biosensor-physik.de/biosensor/](http://web.archive.org/web/*/http://www.biosensor-physik.de/biosensor/)  
e.g. root/example.htm --> <http://www.biosensor-physik.de/biosensor/example.htm>
1. Balck, F., G. Engelsing, (2014) Radiästhetische Beobachtungen bei technischen Geräten- Praktische Erfahrungen und Anwendungen. Wetter-Boden-Mensch, Zeitschrift für Geobiologie (2014) 4, S. 4 -16  
root/wbm-seminar-odenwald-2014-03-low.pdf
  2. Balck, F., (2016a) Radiästhesie als wichtiges Werkzeug für physikalische Experimente, Messen ohne technische Geräte mit sensitiven Personen - Teil 1, Wetter-Boden-Mensch, Zeitschrift für Geobiologie (2016) 2, 24-41  
root/wbm-2016-teil01.pdf
  - 2a. Balck, F. Radiesthetics as an important tool for physical experiments Part 1. Measurements by sensitive persons without the use of technical equipment  
root/wbm-2016-teil01-english.pdf
  3. Balck, F., (2016b) Radiästhesie als wichtiges Werkzeug für physikalische Experimente, Praktische Beispiele - einfache Versuche zum Selbermachen - Teil 2, Wetter-Boden-Mensch, Zeitschrift für Geobiologie (2016) 3, 6-27  
root/wbm-2016-teil02.pdf
  - 3a. Balck, F., Radiesthetics as an important tool for physical experiments Part 2. Practical examples – simple experiments which anyone can perform  
root/wbm-2016-teil02-english.pdf
  4. Keen, J. (2010a) The Causes of Variations When Making Dowsable Measurements; Part 4- The Effects of Geometric Alignments and Subtle Energies, 7 January, e-paper online at <http://vixra.org/abs/1001.0004>
  - 4a. Keen, J. (2010b) Is Dowsing a Useful Tool for Serious Scientific Research? World Futures: Taylor & Francis - The Journal of General Evolution 66(8): S. 557-572.
  5. Krinker M., L. Pismenny (2006) What stands beyond Dowsing and Feng Shui, New York, ISBN 978-5-85051-406-8
  6. Reddish, V.C. (1998) Dowsing physics: interferometry, Transactions of the Royal Society of Edinburgh-Earth Sciences Vol 89, 1-9
  - 6a. Reddish, V.C., R.J. Dodd, J.W. Harrish, C.M. Humphries, (2002), Towards a physics of dowsing: inverse effects in northern and southern hemispheres, Transactions of the Royal Society of Edinburgh-Earth Sciences Vol 93, 95-99
  7. Volkamer, K. Detection of Dark-Matter-Radiation of Stars During Visible Sun Eclipse Nuclear Physics B (Proc. Suppl.) 124 (2003) 117-127
  - 7a. Volkamer, K. Feinstoffliche Erweiterung unseres Weltbildes, Weißensee-Verlag, Berlin, (2009) ISBN 978-3-89998-133-9
  8. Balck, F., (1) root/rosenquarz.htm, 9. Balck, F., (2) root/quarzzrohr-angeregt.htm
  10. Balck, F., (3) root/kuehlwasser-vier-01.htm 11. Balck, F., (4) root/stromleiter-rotierend.htm
  12. Balck, F., (5) root/rotierende-magnetfelder.htm 13. Balck, F., (6) root/led-stress.htm